

Contrast Enhancement of Portal Images with Adaptive Histogram Clip

Georgi Gluhchev

Institute of Information Technologies, 1113 Sofia

1. Introduction

The radiotherapy is a widely used and effective method for cancer treatment where a high-energy beam is targeted at the tumor volume. To properly deliver the required radiation to the tumor and to prevent surrounding tissue from destruction, the beam has to be shaped as prescribed by the physician. This requires registration of two images: a reference image and an image obtained during the radiation delivery called portal image. However, portals are notorious with their poor quality which hampers the anatomical structure delineation and makes image comparison a challenge. Therefore, the accurate registration requires a preprocessing step aimed at the contrast enhancement.

Many contrast enhancement techniques are based on the histogram equalization (HE). The idea is to transform the distribution function of the original image and make it as close as possible to a distribution of prescribed shape. As a result some grey levels are combined into one bin and the dynamic range may increase. However, when applied to a whole image HE will ignore local peculiarities and may not perform very well. To avoid this an adaptive histogram equalization technique (AHE) was developed [1, 2]. Here HE is applied in a window sliding over the image pixel by pixel and the grey level of the central window pixel is transformed, accordingly. This technique performs better than HE but at the expense of much more computational time. To reduce it, an interpolated AHE was developed by Pizer et al. [3]. In their approach the image is divided into $n \times n$ contextual regions of size $d \times d$ and histograms are evaluated and equalized for all regions. The greys of the original image are transformed using a bilinear interpolation of the equalized histograms of every four neighbor regions. A slightly different approach was suggested in [5]. While the obtained quality is almost as good as that obtained by AHE, the processing time is significantly reduced. A major shortcoming of these approaches concerns the overenhancement of relatively homogeneous regions. Thus, the noise in the background of portal images may be drastically increased. Also, field edges may be significantly blurred.

To reduce the noise enhancement and distortion of the radiation field edge, a contrast limited adaptive histogram equalization (CLAHE) has been suggested by S. M. Pizer et al. [4]. The idea is to clip histograms from the contextual regions before equalization. Thus the influence of dominant grey levels will be diminished. The magnitude of the clip permits to trade off contrast enhancement for noise increase. However, a constant clip value applied to the entire image may not be appropriate. For example, contrast enhancement is not necessary outside the field. Also, contrast enhancement may not be welcome for the contextual regions where the field edge goes through because the edge may be severely distorted.

An approach aimed at the adaptation of clipping level all over the image was published by Y. Bao [6]. The author introduces a function

$$(1) \quad H_c = H(\sigma) m,$$

where m and σ are the mean value and standard deviation of the greys from the contextual region, respectively, and $H(\sigma)$ is a predefined function in σ . The magnitude of the clipping factor is suggested to be proportional to H_c . When applied to portal images this technique does not perform very well. This is due to the fact that H_c is usually high at the boundary which leads to a significant edge blur. In an attempt to avoid this we have developed an approach that recognizes contextual regions R_i as belonging to the background, field and field edge. This permits to assign different clip levels for the three types of regions.

2. Identification of contextual regions

To obtain a good image quality, small clipping values have to be attached to homogeneous regions, thus preventing from much noise in the background. Also, small values are required for boundary regions in order to reduce the edge blur, while large values are required for the regions inside the field. To achieve this, contextual regions R_i have to be recognized as belonging to the background, boundary and inner part of the field, respectively.

2.1. Definition of contextual regions

Three types of contextual regions R_i are defined in the parameter space (m, σ) as follows:

- a) **B** – at least 90% of pixels in the region are from the background;
- b) **F** – at least 90% of pixels in the region are from the field;
- c) **E** – all regions different from **B** and **F**.

Types **B**, **F** and **E** are characterized with different values of m and σ . For instance, regions from **B** will have small m_i and σ_i , regions from **F** will have average m_i and average or relatively small σ_i , while regions from **E** will have average m_i and relatively large σ_i . This is shown in Fig. 1 where parameters (m, σ) are obtained from a real portal image of a patient treated in the Head & Neck. The ROI (Region Of Interest) was divided into contextual regions R_i of size 32×32 pixels. To classify them into groups **B**, **F** and **E**, first, the field contour was automatically detected [7] and second, conditions a), b) and c) were checked for every R_i . The black squares in Fig. 1 represent regions of type **B**, black triangles show regions of type **F** and open squares are used for edge regions **E**.

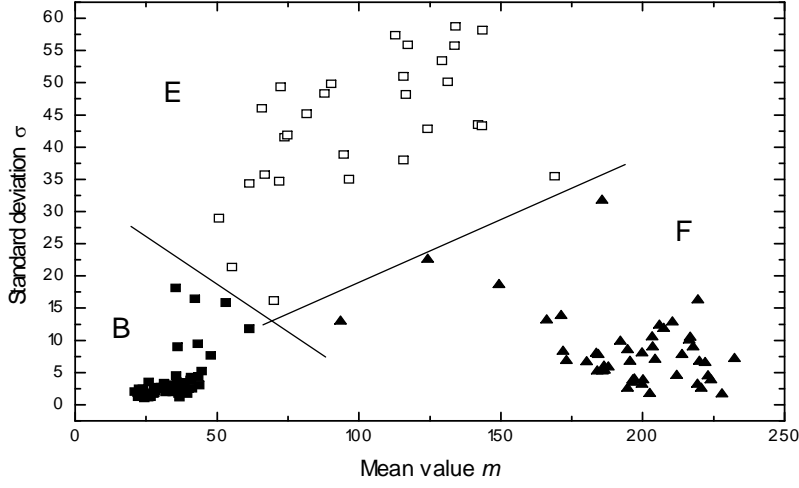


Fig. 1. Clusters corresponding to the background regions (B), field regions (F) and edge regions (E)

2.2. Clustering procedure

In Fig. 1 types **B**, **F** and **E** of regions are properly separated with straight lines which suggests that an automatic classification may be used to identify the region's type. For this a clustering technique may be applied. However, in case of different spread of the clusters Euclidean distance may not be an appropriate measure of the similarity between points in the parameter space. Instead, metric tensors are used based on the evaluation of the inverse covariance matrices Σ_K^{-1} of the corresponding clusters.

Let

$$(2) \quad \Sigma_K^{-1} = \begin{vmatrix} a_{11}^K & a_{12}^K \\ a_{21}^K & a_{22}^K \end{vmatrix}$$

be the inverse covariance matrix and $M_K(m_{K0}, \sigma_{K0})$ be COG (Center Of Gravity) of the cluster K ($K = \mathbf{B}, \mathbf{F}, \mathbf{E}$). The distance d_{iK} between point $R_i(m_i, \sigma_i)$ and cluster K is defined by the formula

$$(3) \quad d_{iK} = (m_i - m_{K0}, \sigma_i - \sigma_{K0}) \begin{vmatrix} a_{11}^K & a_{12}^K \\ a_{21}^K & a_{22}^K \end{vmatrix} \begin{pmatrix} m_i - m_{K0} \\ \sigma_i - \sigma_{K0} \end{pmatrix}.$$

The clustering algorithm looks like this.

1. Select starting points S_K for $K = \mathbf{B}, \mathbf{F}, \mathbf{E}$. For this following suggestions may be used (see Fig. 1):

S_B is the point with $m = \min_j(m_j)$,

S_F is the point with $m = \max_j(m_j)$,

S_E is the point with $\sigma = \max_j(\sigma_j)$.

2. Set $M_K = S_K$.

3. Evaluate distance d_{ik} between point (m_i, σ_i) and point M_k for all regions R_i and all k .

4. Assign region R_i to the cluster with minimal distance d_{ik} .
After this step the regions will be redistributed between clusters.

5. Evaluate new COG for the clusters. If the new COG are different from COG evaluated at the previous iteration, go to step 3, otherwise clustering is completed.

This procedure usually converges to a single region distribution between clusters. The distribution does not depend on the starting points but the number of iterations may significantly depend on it.

2.3. Clipping level selection

Now then the contextual regions have been identified, clipping values have to be assigned to them depending on the type they belong to. The **B** regions do not need contrast enhancement at all and $c = 1$ has to be selected for them. For **E** regions a trade off is required between the enhancement of the useful information from the field and preservation of the field edge, therefore $1 < c < 3$ is recommended. The **F** regions may be assigned a large clip level having in mind that large c will increase the noise as well.

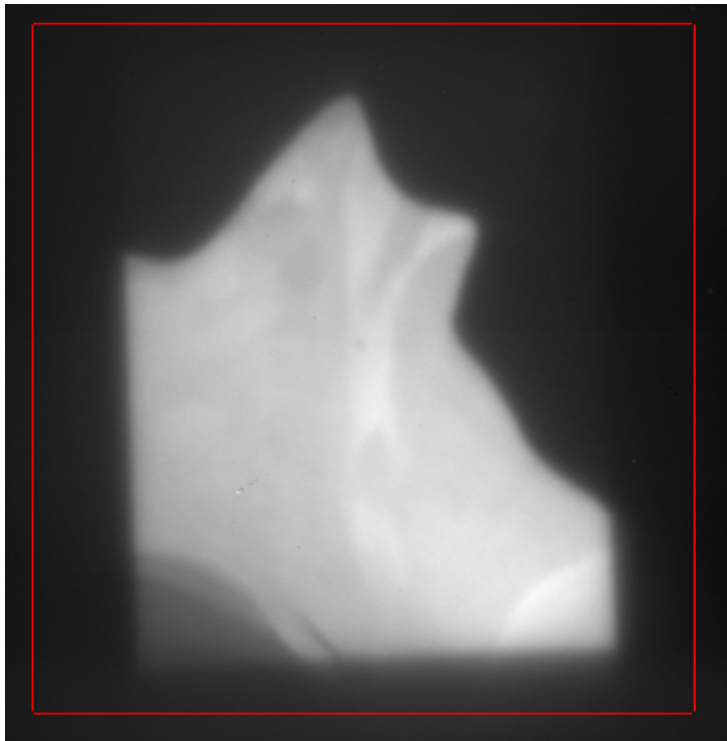
3. Experimental results

Experiments with real portal images from different sites have been carried out to check the accuracy of the cluster algorithm and the effect of different clip levels. The following metric tensors were used for the three types of regions:

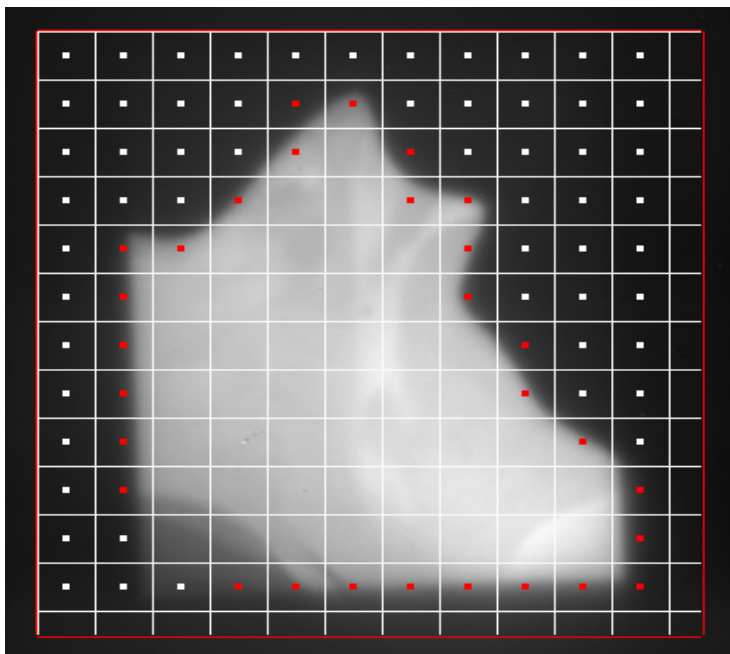
$$\Sigma_B^{-1} = \begin{vmatrix} 0,0268 & -0,331 \\ -0,0331 & 0,1045 \end{vmatrix}, \quad \Sigma_F^{-1} = \begin{vmatrix} 0,0018 & 0,00353 \\ 0,00353 & 0,0384 \end{vmatrix}, \quad \Sigma_E^{-1} = \begin{vmatrix} 0,0029 & -0,0012 \\ -0,0331 & 0,019 \end{vmatrix}$$

Figures 2 b-d show the result of processing of a portal image of a patient treated in the Head & Neck. The original image is shown in Fig. 2a. Fig. 2b shows the selected ROI, contextual regions of size 32×32 pixels and the three types of regions marked with different color. Contrast enhanced images with constant clip $c = 7$ and adaptive clip with $c_B = 1$, $c_E = 2$ and $c_F = 7$ respectively are presented in Fig. 2c and Fig. 2d. While the noise in the background is increased and the field edge is significantly distorted in Fig. 2c, no such effects are visible in Fig. 2d.

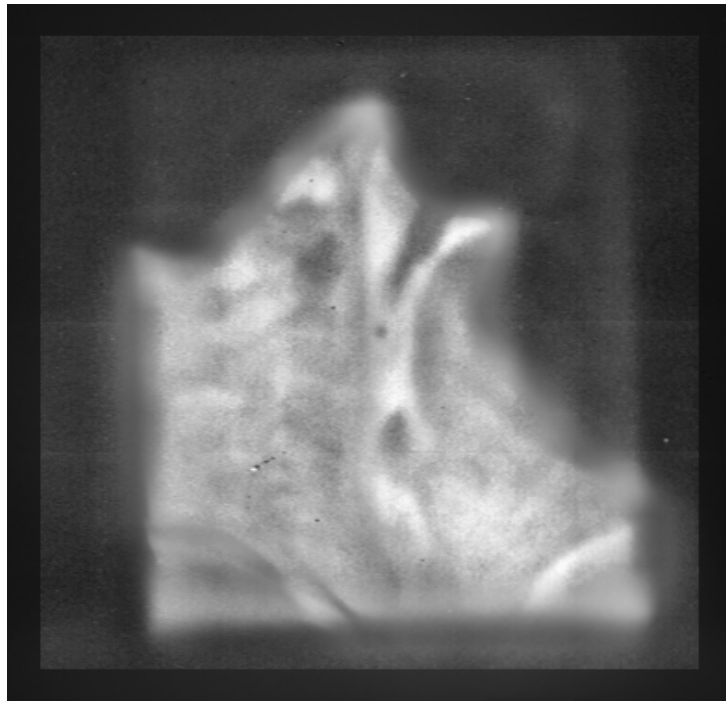
The clustering procedure was able to properly identify contextual regions. There were no misclassifications of field regions for the Head & Neck image which is difficult one because of the unclear field edge in the bottom-left part of the field. No more than 5 iterations were required to find the three clusters of regions. The experiments have proved the good performance of this approach.



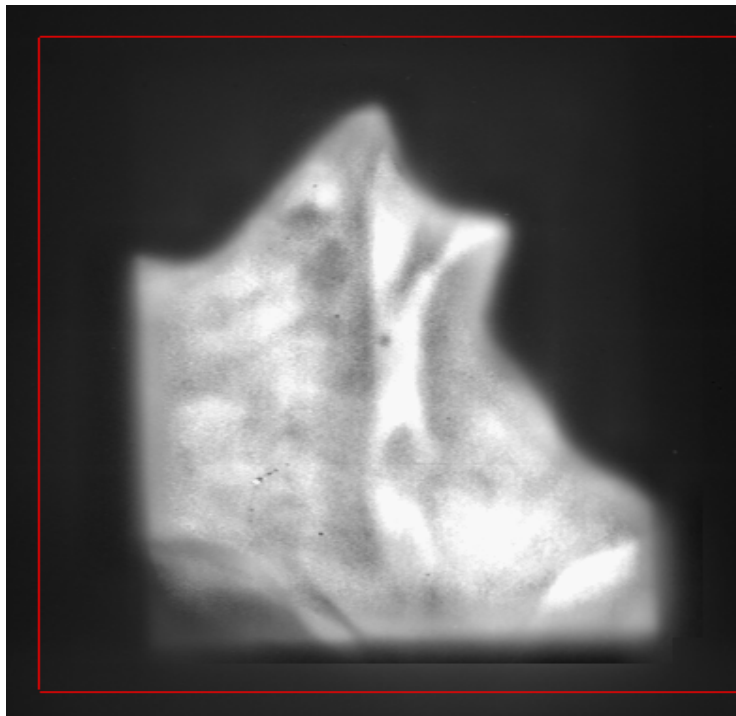
a)



b)



d)



d)

Fig. 2. a) Original H&N image, b) Marked image, c) Constant clip, d) Adaptive clip

4. Conclusion

We have developed an approach aimed at the contrast enhancement of portal images without noise enhancement outside the radiation field and without severe distortion of the field edge. A cluster procedure was used that proved to be robust, accurate and fast. It does not depend neither on dynamic characteristics of images nor on the initial selection of cluster points.

Acknowledgments

This work was partly supported by the Manitoba Cancer Treatment and Research Foundation and Siemens Medical Systems Inc.

References

1. Ketchman, D. J., R. W. Lowe and J. W. Weber. Real-time image enhancement techniques. – In: Seminar on Image Processing, 1976, 1–6.
2. Hummel, R. A. Image enhancement by histogram transformation. – Comput. Graphics and Image Processing, **6**, 1976, 184–197.
3. Pizer, S. M., J. B. Zimmerman and E. V. Staab. Adaptive grey level assignment in CT scan display. J. Comput. Assisted Tomography, **8**, **2**, 1984, 300–305.
4. Pizer, S. M., E. P. Amburn, J. D. Austin et al. Adaptive histogram equalization and its variations. – In: Comput. Vision, Graphics and Image Proc., **39**, 1987, 355–368.
5. Leszczynski, K. W., S. Shalev. A Robust Algorithm for Contrast Enhancement by Local Histogram Modification. Image & Vision Comput., 1989, 205–209.
6. Bao, Y. A novel histogram modification approach for medical image enhancement. – SPIE, Vol. 2167, Image Processing, 1994, 755–765.
7. Gluchev, G., S. Shalev. Fast algorithm for radiation field edge detection. – SPIE, Vol. 1898, Image Processing, 1993, 126–133.

Улучшение портальных изображений с помощью адаптивного гистограммного клиппирования

Георги Глухчев

Институт информационных технологий, 1113 София

(Резюме)

Описывается новый подход для улучшения контраста портальных изображений. Контекстуальные области классифицируются в кластеры **В**, **Ф** и **Е**, соответствующие фону, полю и контуру поля. Специфическое значение клиппирования присваивается каждому кластеру до гистограммной эквализации. Эксперименты с портальными изображениями показали эффективность этого подхода.